

On the Simulation of Low-Frequency Noise Upconversion in InGaP/GaAs HBTs

Matthias Rudolph, *Senior Member, IEEE*, Friedrich Lenk, *Member, IEEE*, Olivier Llopis, and Wolfgang Heinrich, *Senior Member, IEEE*

Abstract—Residual phase-noise measurements of GaAs heterojunction bipolar transistors (HBTs) with different low-frequency noise properties are used to investigate how accurate a compact HBT model can predict the upconversion of low-frequency noise under nonlinear operation. We find that the traditional low-frequency source implementation, as well as a cyclostationary noise source implementation, have shortcomings under different operation conditions. While, in general, the cyclostationary approach yields much better results, it fails under certain operation conditions. Experimental evidence is given that this is caused by overestimated correlation between baseband noise and RF noise sidebands. It is shown that a model based on cyclostationary sources with reduced cross-correlation yields good agreement between measurement and simulation in all cases.

Index Terms—Amplifier noise, burst noise, equivalent circuit, heterojunction bipolar transistor (HBT), noise, oscillator noise, phase noise, semiconductor device modeling, semiconductor device noise, shot noise.

I. INTRODUCTION

THE QUESTION of how the low-frequency noise sources in semiconductor devices contribute to the noise spectrum under nonlinear operation is still a subject of intensive research. In linear operation, they cause $1/f$, burst, or flicker noise with a single-pole low-pass spectrum, Lorentzian-like or $1/f^\alpha$ shaped. In the nonlinear regime, however, this low-frequency noise is converted to high frequencies due to mixing processes. Most prominent is the contribution to the phase noise of oscillators, where the low-frequency noise dominates the spectrum close to the carrier [1].

At the device level, noise descriptions for the small-signal regime are well established in transistor models. In the large-signal case, however, it is still a subject of discussion how these sources are to be described correctly. The main extension over the small-signal assumption refers to noise sources, which depend on bias. Under large-signal operation, namely, the current or voltage controlling the noise, the power level is no longer identical to the (time invariant) dc-bias value, but now consists of a time-varying signal with often high harmonic content.

There has been a good deal of work in the literature on this subject, both from the fundamental point-of-view [2]–[6] and

with regard to noise description in circuits [7], [8], primarily oscillators. The purpose of this paper is to link those results to a special class of transistors, the GaAs heterojunction bipolar transistor (HBT), providing both original experimental data and advancing the modeling approach. This paper is organized as follows. In Section II, the basics of large-signal noise descriptions are reviewed focusing on the GaAs HBT case. Section III then addresses the HBT noise model. In Section IV, the HBT devices-under-test are presented, followed by a description of the measurement conditions in Section V. Finally, Section VI presents measurement and simulation results and discusses the consequences.

II. HBT LARGE-SIGNAL NOISE DESCRIPTION

The bias-dependent noise sources in the HBT are functions of the collector current. Therefore, treating the HBT as a nonlinear electrical system, the basic question regarding nonlinear noise description reads: Will the noise sources follow the dc current only, or will it be the instantaneous current? While the first alternative leaves the spectrum of the noise sources unchanged, the second one results in mixing of low-frequency noise with the large-signal current. Thereby, noise sidebands are generated even without any mixing process external to the noise source.

To include the latter case, the common noise description has to be extended. A low-frequency noise source, for instance, is not fully characterized only by its baseband noise spectral density S_{bb} in the large-signal case. Additionally, the noise-sideband spectra at the harmonics, as well as the interfrequency cross-correlation terms between them, have to be specified. This can be written in the form of a sideband correlation matrix, which, in case of a single harmonic signal, reads

$$C = \begin{pmatrix} S_{bb} & S_{bf} \\ S_{bf}^* & S_{ff} \end{pmatrix} \quad (1)$$

with the baseband noise spectrum S_{bb} , the noise sideband at the fundamental frequency S_{bf} , and the interfrequency cross-correlation S_{bf} . If higher harmonics are present, additional terms S_{nfnf} and the corresponding cross-correlation information have to be included. Thus, for N harmonics, C becomes a matrix of rank $N + 1$.

The most critical issue in nonlinear HBT noise description is the low-frequency $1/f$ noise source, usually considered as a noise current source between base and emitter, with a power spectral density being a function of the emitter current. At first glance, it is not obvious why such a noise source that shows a distinct low-pass behavior should be controlled by the instantaneous current. It would mean that the physical process causing

Manuscript received November 12, 2006; revised March 3, 2006.

M. Rudolph, F. Lenk, and W. Heinrich are with the Ferdinand-Braun-Institut für Höchstfrequenztechnik, D-12489 Berlin, Germany (e-mail: rudolph@fbh-berlin.de).

O. Llopis is with the Laboratoire d'Analyse et d'Architecture des Systèmes du Centre National de la Recherche Scientifique, 31 077 Toulouse, France, and also with the University Paul Sabatier, 31 077 Toulouse Cedex 4, France.

Digital Object Identifier 10.1109/TMTT.2006.877055

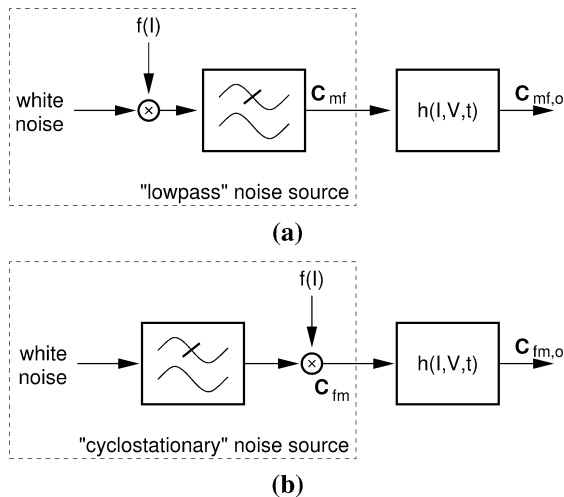


Fig. 1. Schematics illustrating the behavior of low-frequency noise under large-signal excitation. (a) Low-pass noise and (b) cyclostationary noise are transferred through the device by a possibly nonlinear function $h(I, V, t)$.

the noise follows fast changes of the signal, and one would expect white noise from such a fast process, not a $1/f$ -type spectrum. However, more detailed investigations show that this is not contradictory. For example, it has been pointed out that the basic physical process responsible for generation-recombination noise (i.e., the transition of electrons between different energy levels) is, in fact, a white noise process. The low-pass characteristics are observed only when expressing this random process in terms of fluctuations in carrier number or current in the device [9], [10].

Beyond this, various authors have investigated the generation of noise sidebands from low-frequency noise sources using physical device simulation [2]–[6]. As a result, one can conclude: observing $1/f$ -type noise characteristics at the device level does not necessarily mean that the physical process generating this noise has a low-pass behavior. In other words, it is not clear *a priori* that a $1/f$ noise source is of the low-pass type and, thus, cannot follow fast variations in the controlling current. Instead, this question has to be clarified by experimental investigations.

In equivalent-circuit based models, noise is represented by lumped noise sources. Fig. 1 shows schematics of two possible implementations [3]. In the traditional approach [see Fig. 1(a)], the noise level is determined as a function of current $f(I)$, and the resulting noise signal is low-pass filtered. Hence, only the baseband spectrum S_{bb} exists, while the other elements of the sideband correlation matrix are all equal to zero. We refer to this type as to a “low-pass” source. In the case of the implementation shown in Fig. 1(b), on the other hand, a constant low-frequency noise is multiplied with a function of current $f(I)$. Hence, noise sidebands will be observed at all harmonics of the current function $f(I)$, even if the device is still in linear operation. In this case, all elements of the sideband correlation matrix are different from zero. This implementation is commonly referred to as “cyclostationary.” These two cases illustrate two extreme situations. This does not mean, however, that they occur in reality in their pure form. One should remember that the noise sources in a compact transistor model are the result of integrating the contributions of all microscopic sources, which are

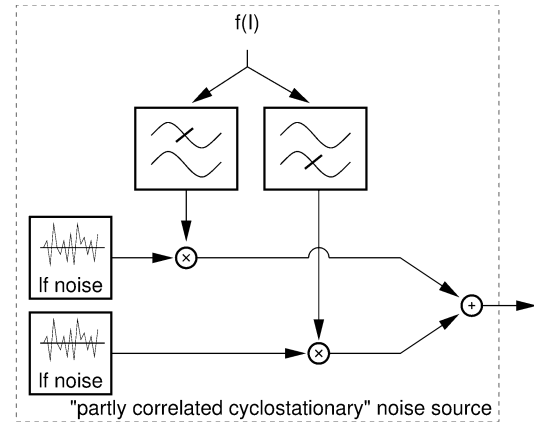


Fig. 2. Schematic showing implementation of the partly correlated cyclostationary noise source. Baseband noise S_{bb} and RF noise sideband S_{ff} are derived from different low-frequency noise sources, which are correlated by an arbitrary value.

transformed through a nonlinear system to the port or branch where the lumped equivalent noise source is located. Therefore, it can be expected that the resulting noise source is neither purely low-pass, nor purely cyclostationary.

Bonani *et al.* compared physical simulations and a compact model for a homogeneous semiconductor sample [3] and a pn diode [5], [6]. Indeed, they found that, in general, it is not *a priori* sure whether a low-pass or a cyclostationary source will be the better approximation. Furthermore, even if the baseband and upconverted noise levels are predicted with decent accuracy, this might not hold true for the interfrequency cross-correlation terms.

The latter observation points at a weakness of the cyclostationary description according to Fig. 1(b). Due to the simple multiplication, all noise sidebands are correlated. Since according to [3]–[6] this is not necessarily true, we need to modify the cyclostationary description of Fig. 1(b) in a way to allow a degree of freedom in the definition of the sideband correlation matrix. For this purpose, we introduce a “partly correlated cyclostationary” noise source implementation, as shown in Fig. 2. The implementation is similar to the cyclostationary source, but the noise sidebands of the harmonics are generated independently from the baseband noise. The current that excites the noise source is split into its dc and RF component. Two low-frequency noise sources, for which an arbitrary correlation can be specified, are then multiplied with these current components. One of them yields the baseband noise S_{bb} , the other one the noise sidebands around the RF signal S_{ff} . Hence, the correlation between the low-frequency noise sources determines the interfrequency correlation S_{fb} . This implementation is identical to the cyclostationary noise source if the low-frequency noise sources are fully correlated.

Recent empirical studies of low-frequency field-effect transistor (FET) [7] and GaAs HBT [8] noise showed that at least some of the noise sources in compact models are to be implemented as cyclostationary sources. The traditional low-pass description did not yield satisfactory agreement with measured mixer or oscillator phase-noise data.

In this paper, we investigate the implementation of low-frequency noise sources in a compact large-signal model for GaAs

HBTs. The devices-under-test were fabricated using the 4-in InGaP/GaAs HBT process line of the Ferdinand-Braun-Institut für Höchstfrequenztechnik (FBH), Berlin, Germany [11]. We measure the residual phase noise, i.e., the noise upconversion mechanisms, in an open-loop configuration with the transistor being operated as an amplifier. These measurements were performed at the Laboratoire d'Analyse et d'Architecture des Systèmes du Centre, National de la Recherche Scientifique (LAAS-CNRS), Toulouse, France [12].

The benefit of this approach over the analysis of oscillator circuits is the reduced complexity and the unambiguous way the measurement data can be related to noise generation inside the HBT. We treat the full phase-noise spectrum for a range of input power and source resistance, which, to the best of the authors' knowledge, has not been published thus far.

It will be shown that using cyclostationary sources significantly improves the accuracy of the phase-noise simulation, while relying on low-pass sources yields unacceptable results in most cases. This is in line with recent publications [8]. However, we will show for the first time that even the model based on lumped cyclostationary sources fails under certain conditions. Evidence is given that this behavior is due to the fact that lumped cyclostationary sources overestimate the correlation between the noise sidebands at the harmonic frequencies and the baseband low-frequency noise. This is the reason why we need a description with variable correlation between the noise spectra at different harmonics according to Fig. 2.

III. HBT NOISE MODEL

The large-signal model employed is the FBH model developed for GaAs-based HBTs [16], [17]. The equivalent circuit including noise sources is shown in Fig. 3. All resistances R_b , R_{b2} , R_e , and R_c exhibit thermal noise at the actual junction temperature T_j . Shot noise is included by two correlated noise sources according to [18]. The base-emitter shot-noise current is driven by I_{be} , and the collector-emitter shot-noise current is driven by $I_f = \beta_f I_{be}$. The correlation time constant is approximated by the constant time-delay parameter T_f of the large-signal model. This simplification does not impact the accuracy of the noise simulation since the HBT is operated at only 3.5 GHz, which corresponds to 10% of f_t , where the correlation is still of minor importance [18].

The shot noise sources read

$$\begin{aligned} \langle |i_b|^2 \rangle &= 2q\Delta f \left(I_{be} + |1 - e^{-j\omega T_f}|^2 I_f \right) \\ \langle |i_c|^2 \rangle &= 2q\Delta f I_f \\ \langle i_b i_c^* \rangle &= 2q\Delta f (e^{j\omega T_f} - 1) I_f \end{aligned} \quad (2)$$

with the electron charge q and the noise bandwidth Δf . The low-frequency noise model has two noise sources [19]. The first one is the noise-current source in parallel with the base-emitter junction

$$\langle |i_{nfb}|^2 \rangle = \Delta f \left(K_{fb} \frac{I_{be}^{A_{fb}}}{f^{F_{feb}}} + K_b \frac{I_{be}^{A_b}}{1 + (f/F_b)^2} \right) \quad (3)$$

with the fitting parameters K_{fb} , A_{fb} , F_{feb} , K_b , A_b , and F_b .

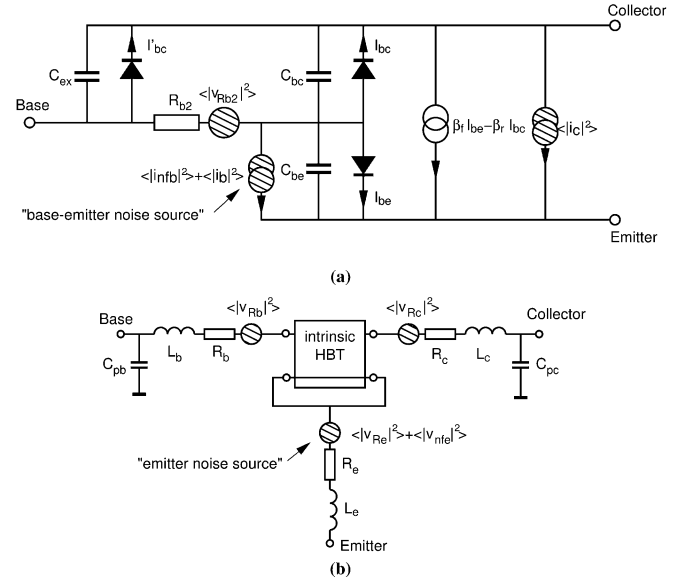


Fig. 3. Large-signal and noise equivalent circuit: (a) intrinsic (b) extrinsic HBT. All resistances contribute thermal noise, $\langle |i_b|^2 \rangle$ and $\langle |i_c|^2 \rangle$ describe shot noise. The sources at the base-emitter junction $\langle |i_{nfb}|^2 \rangle$, and at the emitter resistance $\langle |v_{nfe}|^2 \rangle$ contribute low-frequency noise.

Additionally, the model accounts for a second noise source that describes the Hooge noise contribution of the bulk emitter. Its voltage spectrum is defined as

$$\langle |v_{nfe}|^2 \rangle = \Delta f \left(K_{fe} \frac{(I_{be} + I_f)^{A_{fe}}}{f^{F_{fee}}} \right) \quad (4)$$

with the parameters K_{fe} , A_{fe} , and F_{fee} . In order to allow a comparison of the different possible assumption on the noise sidebands, the low-frequency noise sources are implemented in three different ways, which will be explained in the following for the case of current sources as an example. Noise voltage sources can be handled accordingly.

- *Low-pass noise sources*

The built-in low-frequency noise sources provided by the modeling interface of the circuit simulator (ADS by Agilent Technologies, Palo Alto, CA) are used. These return a baseband spectrum only and are used for the low-pass noise source implementation.

- *Cyclostationary noise sources*

A subcircuit is implemented that forces the simulator to use the instantaneous current when calculating the noise sources in order to obtain a cyclostationary source (see also [7]). Such a noise source generates noise sidebands at large-signal excitation by itself. Fig. 4 shows the circuit setup, which needs a low-frequency noise source and two controlled current sources. In order to obtain a spectrum given by

$$\langle |i|^2 \rangle = \Delta f \left(I^A \cdot \frac{K}{f^\alpha} \right) \quad (5)$$

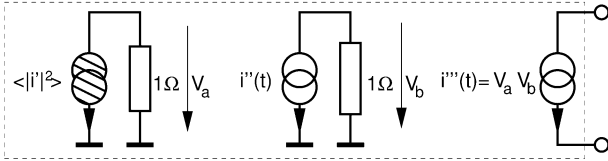


Fig. 4. Cyclostationary implementation of low-frequency noise sources.

with current I , frequency f , and the parameters A , K , and α , the function is split into two parts, i.e., the frequency-dependent noise source

$$\langle |i'|^2 \rangle = \Delta f \left(\frac{K}{f^\alpha} \right) \quad (6)$$

and the current-dependent part

$$i''(t) = \sqrt{IA}. \quad (7)$$

Both current sources are connected to a $1\text{-}\Omega$ resistance in order to access their instantaneous value. The voltage v_a thereby is equivalent to the current $\sqrt{\langle |i'|^2 \rangle}$, while v_b is equivalent to $i''(t)$. Multiplication of these two values by a controlled current source $i'''(t) = v_a \cdot v_b$ yields the desired spectrum.

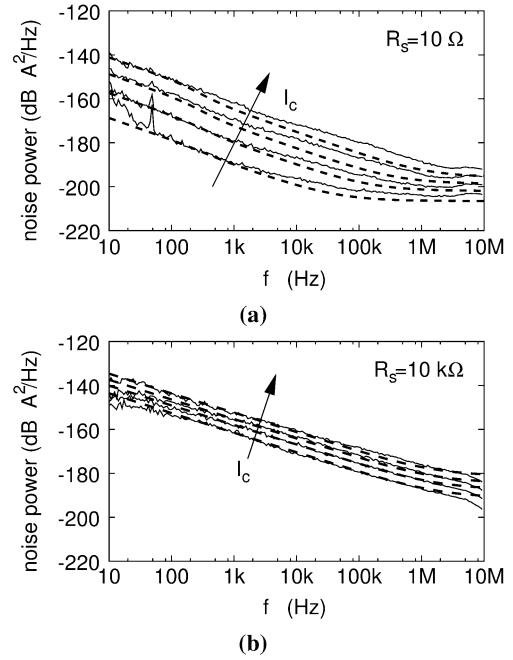
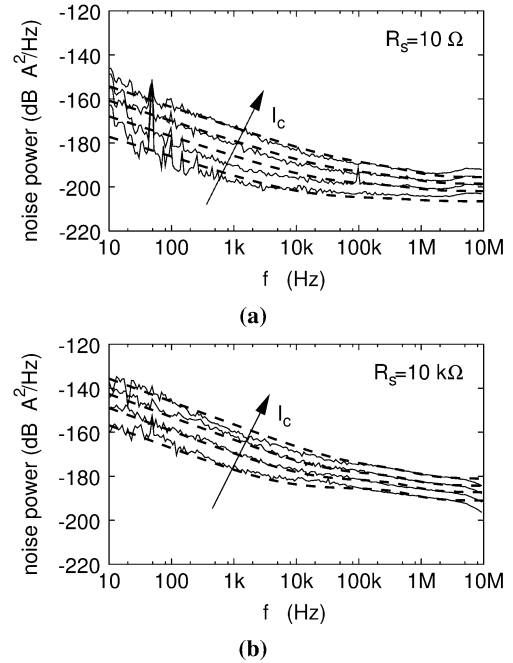
- *Partly correlated cyclostationary noise sources*

In order to allow a variation of the correlation between RF noise sidebands and baseband noise, several cyclostationary sources that are excited by only one harmonic of the large-signal current are connected in parallel. In the case of the measurements under consideration here, only two components, i.e., dc and fundamental frequency, are included. Since the HBT is operated near to linear operation, the second harmonic is approximately 30 dB below the fundamental. The implementation is similar to the cyclostationary source, but the noise sidebands of the harmonics are generated independently from the baseband noise. This requires separated noise sources, and low- and high-pass filtering of the current (see Fig. 2).

In the small-signal regime, the three descriptions are equivalent and no differences are observed. In order to determine the approach best suited in the nonlinear regime, all three approaches are employed and compared.

IV. DEVICES-UNDER-TEST AND LOW-FREQUENCY RESULTS

HBTs with an emitter size of $2 \times 30 \mu\text{m}^2$ from two different wafers were measured. The sole difference between the wafers is that the emitter layer of wafer B was grown in the MOVPE at a temperature that was 20 K higher than that used in the case of wafer A. Both were processed in the same batch, and no difference in the electrical behavior was observed. However, the low-frequency noise is different, as shown in Figs. 5 and 6. The noise was measured with two different source resistances. In the case of a low source impedance (10Ω), the measured collector current is mainly determined by the emitter noise source $\langle |v_{nfe}|^2 \rangle$, while the base-emitter noise source $\langle |i_{nfb}|^2 \rangle$ is almost short circuited. This measurement condition is shown in


 Fig. 5. Low-frequency noise of $3 \times 30 \mu\text{m}^2$ HBT, $V_{cc} = 3\text{V}$, $I_c = 2.5, 5, 10, 20 \text{ mA}$, wafer A. Measurements (solid lines) compared to simulation (broken lines). (a) $10\text{-}\Omega$ source resistance. (b) $10\text{-k}\Omega$ source resistance.

 Fig. 6. Low-frequency noise of $3 \times 30 \mu\text{m}^2$ HBT, $V_{cc} = 3\text{V}$, $I_c = 2.5, 5, 10, 20 \text{ mA}$, wafer B. Measurements (solid lines) compared to simulation (broken lines). (a) $10\text{-}\Omega$ source resistance. (b) $10\text{-k}\Omega$ source resistance.

Figs. 5(a) and 6(a). The emitter noise measured on wafer A is approximately 10 dB higher than that measured on wafer B.

In the case of a high-impedance source ($10 \text{ k}\Omega$), the contribution of the base-emitter noise source is at its maximum, while the emitter noise source is almost of no importance. This measurement condition is shown in Figs. 5(b) and 6(b). The frequency slope of the base-emitter noise measured for wafer

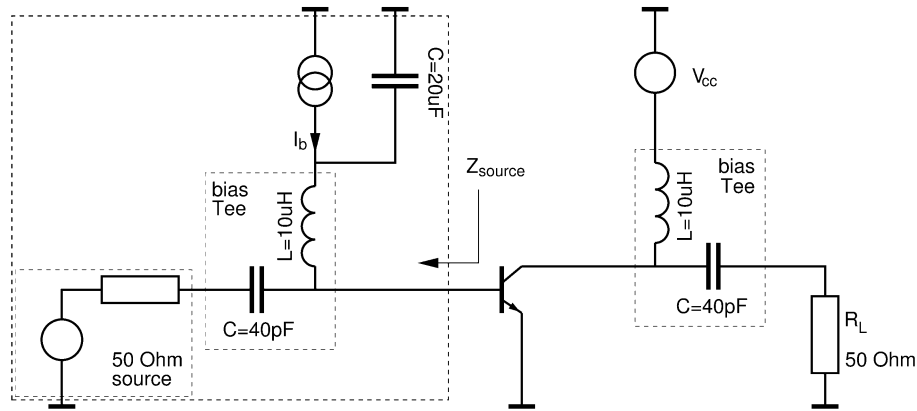


Fig. 7. Circuit setup used for determination of residual phase noise. The source injects powers of $P_{in} = -22, -16, -11, -6$ dBm into the device. The phase noise is measured at the $50\text{-}\Omega$ load resistance. The supply voltage is $V_{cc} = 3$ V, the base current I_b is chosen to obtain $I_c = 30$ mA.

A is less steep than that of wafer B. Also, the current dependence of the noise is less pronounced for wafer A. On the other hand, the noise measured for wafer B contains a component with a Lorentzian spectrum that flattens the noise spectrum above 100 kHz. This component is not observed in the case of wafer A, but it might be shadowed by the generally higher $1/f$ noise level.

It can be concluded that the slightly different growth conditions lead to different Hooke noise in the emitter cap layer [plotted in Figs. 5(a) and 6(a)] and also to different noise of the base–emitter pn junction that is caused mainly by recombination [shown in Figs. 5(b) and 6(b)], although the electrical properties, in general, are not affected.

V. NONLINEAR SIMULATION SETUP

The residual phase-noise measurement setup was presented in [12]. Fig. 7 shows a slightly idealized model for this setup used in the simulation. The HBT under test is operated in a weakly nonlinear power amplifier mode. The residual phase noise, i.e., the noise sidebands of the fundamental tone, are measured at the load resistance R_L . A $50\text{-}\Omega$ source was used to inject input powers of $-22, -16, -11,$ and -6 dBm at 3.5 GHz into the device. The bias tees approximate the characteristics of a commercial device. The values of C and L are not critical with respect to their influence on simulation results in a wide range of values. An ideal current source is used to bias the HBT. Collector bias $V_{cc} = 3$ V is provided by an ideal voltage source.

Phase-noise simulations can be performed either in the time or frequency domain [13]–[15]. In this study, we rely solely on the commercial harmonic-balance circuit simulator ADS 2003 C by Agilent Technologies that simulates the residual phase noise based on conversion matrices in the frequency domain. This standard method is also available in other commercial simulation codes. The FBH HBT model [16], [17] is used. The different types of noise sources are implemented into the software using its C-code [20] and Verilog-A [21] interfaces.

In measurement and simulation, a $20\text{-}\mu\text{F}$ shunt capacitor was placed in parallel with the high-impedance current source [12]. Its purpose was to cause the low-frequency source impedance

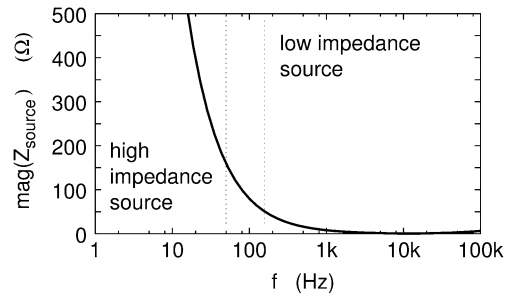


Fig. 8. Simulated magnitude of source impedance at the input of the HBT $|Z_{source}|$ including bias tee (see Fig. 7).

Z_{source} to drop significantly above 100 Hz. Fig. 8 shows simulated values for the magnitude of Z_{source} including bias tee, presented to the HBT according to Fig. 7. The source resistance in the range $f < 50$ Hz, $|Z_{source}| > 150$ Ω will be referred to as the “high-impedance” source, while the range $f > 150$ Hz, $|Z_{source}| < 50$ Ω will be referred to as the “low-impedance” source in the following. The transition frequency is controlled by the value of the shunt capacitor.

VI. RESIDUAL PHASE-NOISE RESULTS

Figs. 9 and 10 present the residual phase-noise measurements together with the simulation results. The data in Fig. 9 refers to wafer A, that in Fig. 10 to wafer B. Simulation results for three types of noise-source implementations are included, i.e., low-pass, cyclostationary, and partly correlated cyclostationary sources.

For both wafers, a model relying on low-pass noise sources underestimates the phase noise (chain-dotted lines in Figs. 9 and 10) and, therefore, is not suited to describe nonlinear noise. In contrast, the model employing cyclostationary sources (dashed lines) shows significantly better results. It should be mentioned that both wafers have one dominant noise source: it is the emitter noise source in the case of wafer A, while it is the base–emitter noise source in the case of wafer B. In fact, neglecting the non-dominant noise source does not change the residual phase-noise result.

However, this approach also fails for some measurement conditions. For wafer A, simulation shows a dip at 150 Hz at

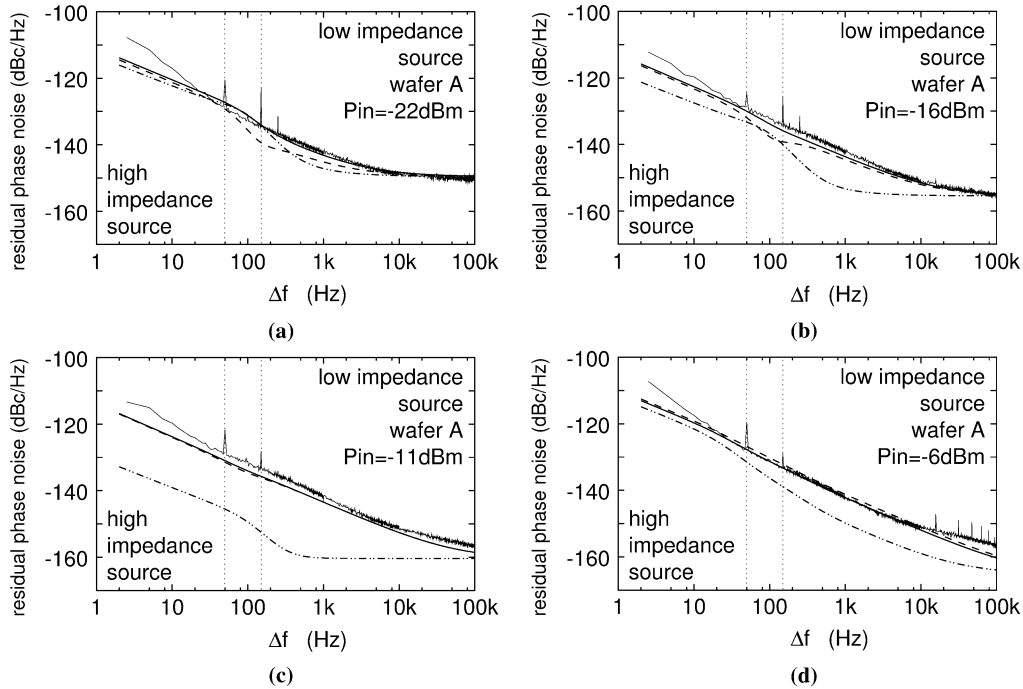


Fig. 9. Double sideband residual phase noise versus frequency offset Δf of a $3 \times 30 \mu\text{m}^2$ HBT on wafer A, input power: (a) $P_{\text{in}} = -22$ dBm, (b) -16 dBm, (c) -11 dBm, and (d) -6 dBm at 3.5 GHz, $V_{\text{cc}} = 3$ V, $I_c = 30$ mA. Measurements compared to simulation: model implementation using low-pass sources ($-\cdot-\cdot-$), cyclostationary sources ($--$), and partly correlated cyclostationary sources with correlation 0.65 ($---$).

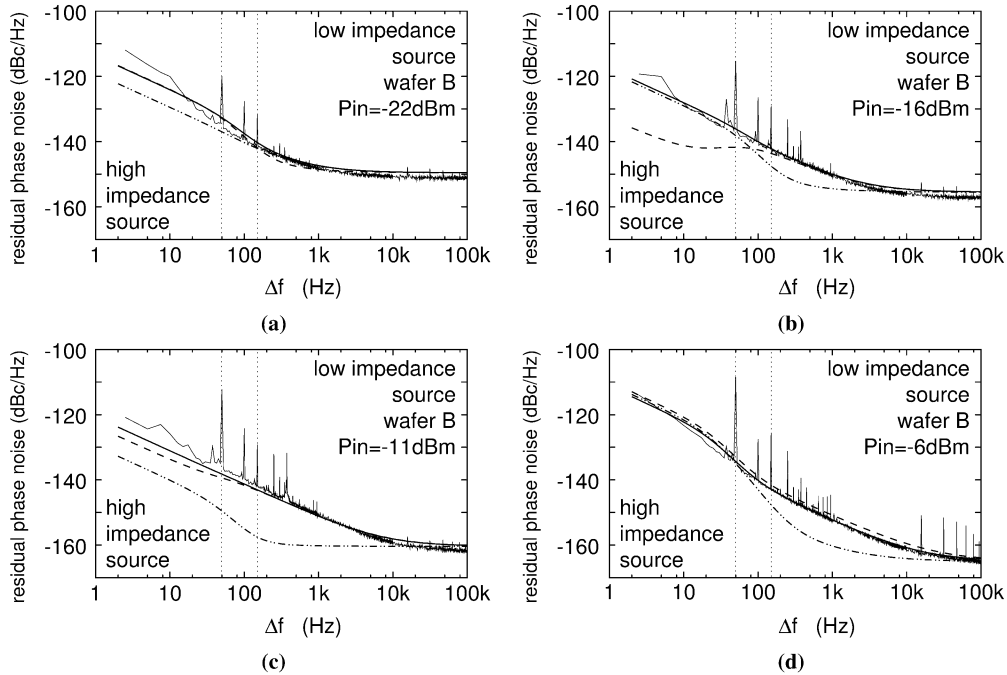


Fig. 10. Double-sideband residual phase noise versus frequency offset Δf of a $3 \times 30 \mu\text{m}^2$ HBT on wafer B, input power: (a) $P_{\text{in}} = -22$ dBm, (b) -16 dBm, (c) -11 dBm, and (d) -6 dBm at 3.5 GHz, $V_{\text{cc}} = 3$ V, $I_c = 30$ mA. Measurements compared to simulation: model implementation using low-pass sources ($-\cdot-\cdot-$), cyclostationary sources ($--$), and partly correlated cyclostationary sources with correlation 0.25 ($---$).

$P_{\text{in}} = -22$ dBm and $P_{\text{in}} = -16$ dBm. For wafer B, the results below 50 Hz are not always satisfying [see Fig. 10(b)], which correlates with the frequency range where the source is of high impedance. At this operation condition, on the other hand, upconversion of the baseband noise due to HBT nonlinearity (i.e., outside the noise sources themselves) is strong. The chain-dotted lines in Figs. 9 and 10 are a measure for this effect.

This is the key to understanding what happens in the critical regions in Figs. 9(a) and (b) and particularly Figs. 10(b) and (c). The low-frequency noise is upconverted by external mixing and interferes with the sidebands of the cyclostationary noise source around the harmonics. Since for the cyclostationary formulation according to Fig. 1(b), the baseband LF noise and that around the higher harmonics are strongly correlated, this interference

may lead to significant cancellation effects. In other words, the noise generated by upconversion (due to device nonlinearity) and that caused by the cyclostationary source cancel each other.

In fact, the noise sidebands of a compact cyclostationary source at dc and harmonics are strongly correlated, which is inherent to the implementation. Hence, reduction of the interfrequency cross-correlation by employing only partly correlated cyclostationary sources can improve simulation accuracy. The optimum fit is achieved for different levels of correlation. In the case of wafer A, the noise sources are still quite strongly correlated (0.65), while this does not apply to wafer B (0.25) (solid lines in Figs. 9 and 10). The differences in the correlation coefficients can be attributed to differences in the dominant noise processes. In the case of wafer A, it has been observed that the phase noise is governed by the emitter noise source, while the base-emitter noise source dominates in case of wafer B. It, therefore, can be expected that different physical noise mechanisms contribute to the overall phase noise with different weights for the two wafers.

VII. CONCLUSIONS

This paper addresses the influence of low-frequency noise sources under nonlinear operating conditions and their implementation in a compact large-signal HBT model. Simulation data is compared to residual phase noise measurements, with the HBT operating in amplifier mode at different power levels, focusing on the phase noise close to the fundamental frequency. Devices-under-test are nominally identical InGaP/GaAs HBTs from the same process run, but with different low-frequency noise levels. Hence, the differences in residual phase noise can be attributed to differences in the low-frequency noise alone.

Thanks to the residual phase-noise measurement, it is possible to analyze the phase-noise generation mechanisms in the HBTs directly. We take into account the full frequency spectrum, different power levels, and the dependence on source impedance. This comprehensive amount of information is presented here for the first time. First, it is shown that a model based on cyclostationary sources is clearly superior to the traditional approach relying on low-pass noise sources. This validates the findings of recently published papers. However, it turns out that under certain conditions (input power level, frequency, and source impedance), the conventional cyclostationary noise model also fails. Experimental evidence suggests that these failures are caused by overestimating the correlation of the noise sidebands in the compact cyclostationary source: the simulated phase noise is significantly too low, even lower than the upconverted baseband noise alone. One finds that using partially correlated cyclostationary sources yields excellent agreement between measurement and simulation for all conditions.

It can be concluded that while the approach based on cyclostationary noise sources commonly yields good results, it does not cover all cases properly. It should be improved by accounting for a variable interfrequency cross-correlation, i.e., not unity, such as assumed for the conventional cyclostationary approach. This also means that predicting phase noise based on

the knowledge of low-frequency noise behavior only is not possible. It requires additional measurements to extract the actual correlation values for a specific device.

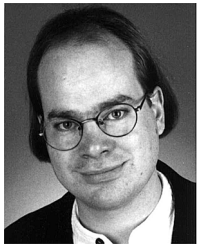
ACKNOWLEDGMENT

The authors would like to thank S. Gribaldo, Laboratoire d'Analyse et d'Architecture des Systèmes du Centre National de la Recherche Scientifique (LAAS-CNRS), Toulouse, France, for performing residual phase-noise measurements, and S. Schulz, Ferdinand-Braun-Institut für Höchstfrequenztechnik (FBH), Berlin, Germany, for performing S -parameter and low-frequency noise measurements.

REFERENCES

- [1] D. Leeson, "A simple model of feedback oscillator noise spectrum," *Proc. IEEE*, vol. 54, no. 2, pp. 329–330, Feb. 1966.
- [2] S. Pérez, T. González, S. L. Delage, and J. Obregon, "Microscopic analysis of generation-recombination noise in semiconductors under DC and time-varying electric fields," *J. Appl. Phys.*, vol. 88, no. 2, pp. 800–807, Jul. 15, 2000.
- [3] F. Bonani, S. D. Guerrieri, and G. Ghione, "Noise source modeling for cyclostationary noise analysis in large-signal device operation," *IEEE Trans. Electron Devices*, vol. 49, no. 9, pp. 1640–1647, Sep. 2002.
- [4] J. E. Sanchez, G. Bosman, and M. E. Law, "Two-dimensional semiconductor device simulation of trap-assisted generation-recombination noise under periodic large-signal conditions and its use for developing cyclostationary circuit simulation models," *IEEE Trans. Electron Devices*, vol. 50, no. 5, pp. 1353–1362, May 2003.
- [5] F. Bonani, S. D. Guerrieri, and G. Ghione, "Compact conversion and cyclostationary noise modeling of pn-junction diodes in low-injection—Part I: Model derivation," *IEEE Trans. Electron Devices*, vol. 51, no. 3, pp. 467–476, Mar. 2004.
- [6] F. Bonani, S. D. Guerrieri, and G. Ghione, "Compact conversion and cyclostationary noise modeling of pn-junction diodes in low-injection—Part II: Discussion," *IEEE Trans. Electron Devices*, vol. 51, no. 2, pp. 477–485, Feb. 2004.
- [7] M. Margraf and G. Böck, "Analysis and modeling of low-frequency noise in resistive FET mixers," *IEEE Trans. Microw. Theory Tech.*, vol. 52, no. 7, pp. 1709–1718, Jul. 2004.
- [8] J.-C. Nallatamby, M. Prigent, M. Camiade, A. Sion, C. Gourdon, and J. J. Obregon, "An advanced low-frequency noise model of GaInP/GaAs HBT for accurate prediction of phase noise in oscillators," *IEEE Trans. Microw. Theory Tech.*, vol. 53, no. 5, pp. 1601–1612, May 2005.
- [9] C. M. Van Vliet, "Macroscopic and microscopic methods for noise in devices," *IEEE Trans. Electron Devices*, vol. 41, no. 11, pp. 1902–1915, Nov. 1994.
- [10] F. Bonani and G. Ghione, *Noise in Semiconductor Devices, Modeling and Simulation*. Berlin, Germany: Springer-Verlag, 2001, pp. 13–23.
- [11] J. Hilsenbeck, F. Lenk, W. Heinrich, and J. Würfl, "Low phase noise MMIC VCOs for Ka -band applications with improved GaInP/GaAs-HBT technology," in *IEEE GaAs IC Symp. Dig.*, 2003, pp. 223–226.
- [12] G. Cibiel, L. Escotte, and O. Llopis, "A study of the correlation between high-frequency noise and phase noise in low-noise silicon-based transistors," *IEEE Trans. Microw. Theory Tech.*, vol. 52, no. 1, pp. 183–190, Jan. 2004.
- [13] F. X. Kaertner, "Determination of the correlation spectrum of oscillators with low noise," *IEEE Trans. Microw. Theory Tech.*, vol. 37, no. 1, pp. 90–101, Jan. 1989.
- [14] A. Hajimiri and T. H. Lee, "A general theory of phase noise in electrical oscillators," *IEEE J. Solid-State Circuits*, vol. 33, no. 2, pp. 179–194, Feb. 1998.
- [15] A. Suárez, S. Sancho, S. Ver Hoeye, and J. Portilla, "Analytical comparison between time- and frequency-domain techniques for phase-noise analysis," *IEEE Trans. Microw. Theory Tech.*, vol. 50, no. 10, pp. 2353–2361, Oct. 2002.
- [16] M. Rudolph, R. Doerner, K. Beilenhoff, and P. Heymann, "Unified model for collector charge in heterojunction bipolar transistors," *IEEE Trans. Microw. Theory Tech.*, vol. 50, no. 7, pp. 1747–1751, Jul. 2002.

- [17] M. Rudolph and R. Doerner, "Consistent modeling of capacitances and transit times of GaAs-based HBTs," *IEEE Trans. Electron Dev.*, vol. 52, no. 9, pp. 1969–1975, Sep. 2005.
- [18] M. Rudolph, R. Doerner, L. Klapproth, and P. Heymann, "An HBT noise model valid up to transit frequency," *IEEE Electron Device Lett.*, vol. 20, no. 1, pp. 24–26, Jan. 1999.
- [19] P. Heymann, M. Rudolph, R. Doerner, and F. Lenk, "Modeling of low-frequency noise in GaInP/GaAs hetero-bipolar transistors," in *IEEE MTT-S Int. Microw. Symp. Dig.*, 2001, pp. 1967–1970.
- [20] "User defined models" Agilent Technol., Palo Alto, CA, Dec. 2003. [Online]. Available: <http://eesof.tm.agilent.com/docs/adsd2003C/pdf/modbuild.pdf>
- [21] "Using Verilog-A in advanced design system" Agilent Technol., Palo Alto, CA, Dec. 2003. [Online]. Available: <http://eesof.tm.agilent.com/docs/adsd2003C/pdf/verilog.pdf>



Matthias Rudolph (M'99–SM'05) received the Dipl.-Ing. degree in electrical engineering from the Berlin University of Technology, Berlin, Germany, in 1996, and the Dr.-Ing. degree from Darmstadt University of Technology, Darmstadt, Germany, in 2001.

He is currently a Senior Scientist with the Ferdinand-Braun-Institut für Höchstfrequenztechnik (FBH), Berlin, Germany. His research is focused on modeling of FETs and HBTs and on the design of power, broadband, and low-noise amplifiers. He authored or coauthored over 40 publications in refereed journals and conferences and *Introduction to Modeling HBTs* (Artech House, 2006).

He is currently a Senior Scientist with the Ferdinand-Braun-Institut für Höchstfrequenztechnik (FBH), Berlin, Germany. His research is focused on modeling of FETs and HBTs and on the design of power, broadband, and low-noise amplifiers. He authored or coauthored over 40 publications in refereed journals and conferences and *Introduction to Modeling HBTs* (Artech House, 2006).



Friedrich Lenk (M'00) was born in Lübbecke/Westfalen, Germany, in 1966. He received the Dipl.-Ing. degree in electrical engineering and Dr.-Ing. from the Berlin University of Technology, Berlin, Germany, in 1995 and 2003 respectively.

He is currently with the Ferdinand-Braun-Institut (FBH), Berlin, Germany. His focus is on modeling and design of monolithic microwave integrated circuits (MMICs) with FET and HBT devices.



Olivier Llopis was born in Albi, France, on March 16, 1965. He received the Diploma of Telecommunications engineer from (ENSTB), Brest, France, in 1987, and the Ph.D. degree in electronics from the University Paul Sabatier, Toulouse, France, in 1991.

He is currently with the Laboratoire d'Analyse et d'Architecture des Systèmes du Centre National de la Recherche Scientifique, Toulouse, France, where he leads the Microwave Team, and more particularly, within this team, the scientific field of optical and microwave systems for signal transmission with low additive noise. His interests are in the study of microwave sources, and more generally, nonlinear circuits, both with theoretical and experimental approaches. He has proposed different techniques to investigate the phase noise in microwave oscillators, and designed ultra-low phase-noise microwave sources. He is now also involved in the development of optical-microwave systems for time and frequency applications. He has authored or coauthored over 100 papers either in scientific journals or international conferences.

He is currently with the Laboratoire d'Analyse et d'Architecture des Systèmes du Centre National de la Recherche Scientifique, Toulouse, France, where he leads the Microwave Team, and more particularly, within this team, the scientific field of optical and microwave systems for signal transmission with low additive noise. His interests are in the study of microwave sources, and more generally, nonlinear circuits, both with theoretical and experimental approaches. He has proposed different techniques to investigate the phase noise in microwave oscillators, and designed ultra-low phase-noise microwave sources. He is now also involved in the development of optical-microwave systems for time and frequency applications. He has authored or coauthored over 100 papers either in scientific journals or international conferences.



Wolfgang Heinrich (M'84–SM'95) received the Dipl.-Ing., Dr.-Ing., and Habilitation degrees from the Technical University of Darmstadt, Darmstadt, Germany, in 1982, 1987, and 1992, respectively.

Since 1993, he has been with the Ferdinand-Braun-Institut für Höchstfrequenztechnik (FBH), Berlin, Germany, where he is the Head of the Microwave Department and Deputy Director of the Institute. His current research activities focus on MMIC design with emphasis on oscillators, GaAs and GaN power transistors, electromagnetic simulation, and millimeter-wave packaging.

Dr. Heinrich served as a Distinguished Microwave Lecturer for the 2003–2005 term. He was chairman of the German IEEE Microwave Theory and Techniques (MTT-S)/Antennas and Propagation (AP) Chapter for the 2002–2006 election period.